Aalborg University

Assessment of the natural convection heat transfer phenomenon on a vertical wall, when waves are added along the wall

MSc Thermal Energy and Process Engineering

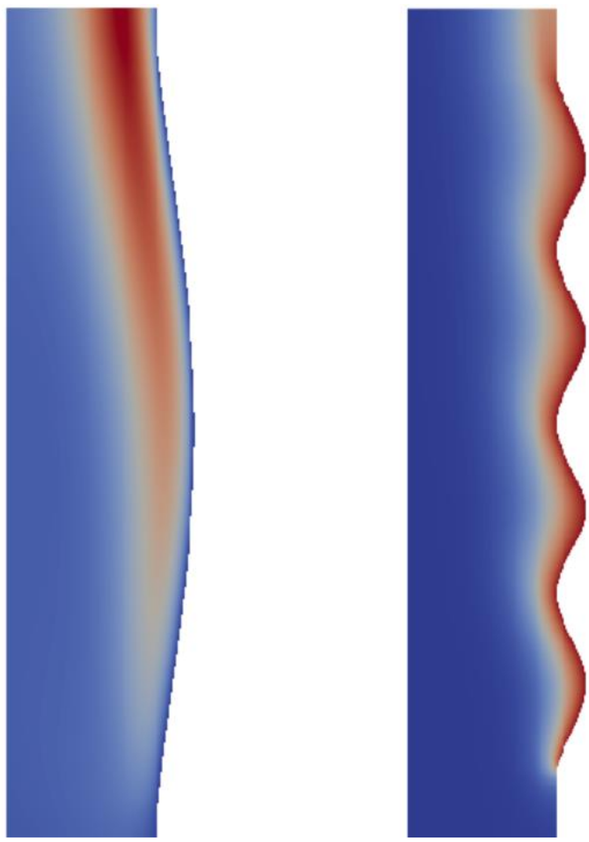

Federico Censi

AALBORG UNIVERSITY
DENMARK

Title:	Assessment of the natural convection heat transfer phenomenon on a vertical wall, when waves are added along the wall.
Project period:	April 2020 to August 2020
ECTS:	30 ECTS
Supervisors:	Henrik Sørensen and Jakob Hærvig
Energy Engineering	Pontoppidanstræde 111 9220 Aalborg

SYNOPSIS:

The evaluation of the natural convection heat transfer phenomenon on a vertical wall is performed, in order to assess if including waves on the vertical wall, is a convenient choice, when an enhancement of the heat transfer rate wants to be achieved. The CFD simulations in this thesis are performed using OpenFOAM, a popular open-source CFD software. To study the variation of the heat transfer rate along the wall, the Nusselt number variation is observed. The Nusselt number gives a precise estimation of the improvement of the heat transfer rate by heat convection, compared to heat conduction. Thus, observing how this value changed along the wall, it was possible to quantify the fluctuation of the heat transfer rate along the different vertical walls assessed. Two investigations are performed, one changing the amplitude of the waves along the wall, and one changing the number of the waves along the wall but keeping fixed the amplitude. It is observed that a local improvement of the heat transfer rate can be achieved only for some areas of the wall, and that this variation is more evident when the amplitude of the wave is changed. But looking at the overall heat transfer rate along the wall, the flat vertical wall has the highest heat transfer rate, compared to the other geometries assessed.

Federico Censi

Pages, total: 49

Preface

This semester project is written by one 4th Semester MSc student on Energy Engineering with Thermal Energy and Process Engineering specialization. The purpose is to analyze the heat transfer natural convection rate of different vertical wall geometries.

Prerequisites

It is expected from the reader to have basic knowledge about thermodynamics and mathematical modelling.

Reading Guide

The equations, figures and tables presented in this report are numbered according to the chapter they belong to. As an example, the numbering of Figure 2.3 indicates that it is the third figure of chapter two. Any of the mentioned objects include a short description of the content of the object.

Each new variable that is presented in an equation is described together with its unit and symbol. All the variables are placed on a list called 'Nomenclature' where abbreviations and subscripts used along the report are also included. These abbreviations are described when they are used for the first time.

Along this report, brackets are used for citations. These citations drive the reader to the bibliography at the end of this report. Each citation gives the main reference about where this information is coming from as the name of the author, website, year of publication, title or dates, depending of the type of source, as they can be books, articles, websites or interviews, etc.

The main softwares used for this report are OpenFOAM® and Paraview®.

Nomenclature

Symbol	Description	Unit
τ	shear stress	[N/m^2]
ρ	Air density	[kg/m^3]
t	Time	[s]
μ	Dynamic viscosity	[N/m^2]
ν	Kinematic viscosity	[m$^2/s$]
k	Turbulence kinetic energy	[m$^2/s^2$]
ϵ	Rate of turbulence dissipation	[s$^2/m^3$]
δ_v	Velocity boundary layer	[m]
δ_t	Thermal boundary layer	[m]
g	Gravitational acceleration	[m/s^2]
β	Volume expansion coefficient	[1/K]
h	Convection heat transfer coefficient	[W/m^2K]
k	Conduction heat transfer coefficient	[W/m^2K]
P	Pressure acting on the surface of the control volume	[Pa]
T_s	Surface temperature	[K]
T_{inf}	Ambient temperature outside the boundary layer	[K]
u	Velocity of the fluid flow	[m/s]

Acronyms

Acronym	Description
CFD	Computational Fluid Dynamic
2D	Two dimensions
PCs	Personal computers
Nu	Nusselt number
Gr	Grashof number
Pr	Prandtl number
RA	Rayleigh number
PIMPLE	PIMPLE algorithm

Table of contents

Part I

Introduction

1 Introduction

The temperature induced buoyant flow is a phenomenon which occurs when a fluid is heated up from a hot surface. When the layers of fluid close to the surface get warmer, the density will decrease and they tend to rise. When there is fluid in motion, the heat transfer between the fluid and the hot surface is defined as convection heat transfer. The object of this thesis is to analyze the natural convection phenomenon for different geometries of a vertical plate, to assess if different configurations are more effective in order to enhance the heat transfer.

Heat exchangers are often used to cool down electronic devices by heat dissipation. In many cases, the heat exchange happens on vertical surfaces, thus it is interesting to study this phenomenon in order to find solutions to enhance the heat transfer. Considered the importance of natural convection heat transfer, many studies have been conducted in order to investigate and quantify the heat transfer for different geometries or for different flow conditions.

1.1 Literature review

In this research Das and Mahmud (2003) investigated the natural convection inside a wavy enclosure. The enclosure consists of two wavy walls, kept isothermal at different temperatures, the Grashof number was kept between 10^3 and 10^7. They noticed that the amplitude-wavelength ratio affects the local heat transfer as well as the flow field, in particular they observed that more significant changes of the value of the local Nusselt number along the wavy enclosure are observed for higher values of Grashof number, but the amplitude-wavelength ratio had no relevant effect on the average heat transfer rate.

The scope of the paper of Tanda (1997) is to simulate the natural convection on a vertical channel, in order to evaluate if the presence of roughness on the vertical wall, affects the heat transfer rate. It is observed that this adjustment leads to a local decreasing of the heat transfer rate just above and below each rib. The author also states that a lower heat transfer is registered for the narrowest ribbed channel, and it concludes that for the parameters studied in that research, adding squared ribs does not improve the heat transfer rate compared to a flat vertical wall.

The article of Hærvig, Jensen, and Sørensen (2019) aims to evaluate the effects of inserting triangular roughness on a vertical wall, in order to enhance the heat transfer rate, a representation of the triangular roughness on the wall can be seen in Fig. 1.1. In the research it is chosen to study different flow conditions, changing the value of the Grashof number. The authors conclude that adding triangular roughness can lead to a local improvement of the heat transfer rate, compared to the natural convection on a flat vertical wall. But comparing the average values of the Nusselt number for the walls with roughness and for the flat one, it is observed that the flat vertical wall has the highest heat transfer rate.

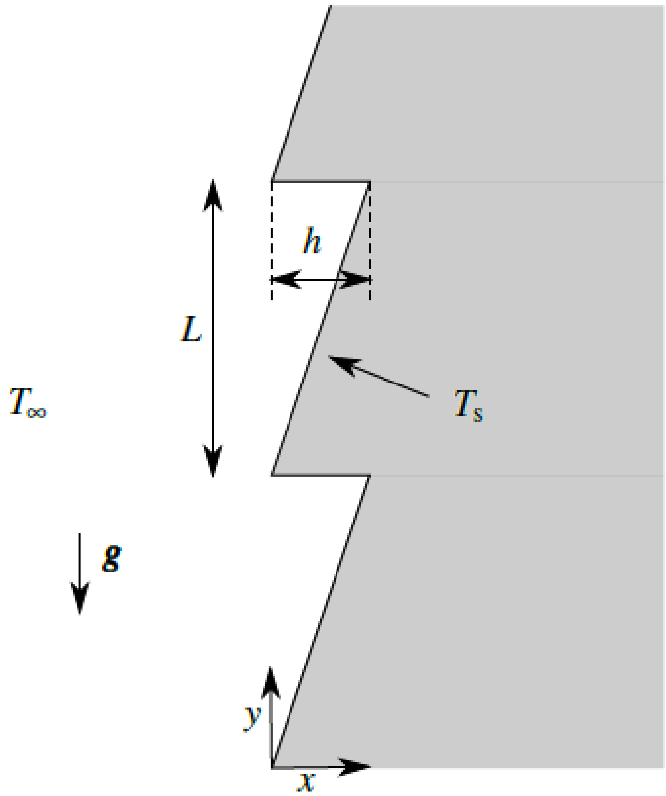

Figure 1.1: *Triangular roughness on a vertical wall (Hærvig, Jensen, and Sørensen, 2019).*

In the article of Kogawa et al. (2016) a comparison between the natural convection heat transfer rate for a flat vertical wall, and the heat transfer rate for two parallel plates is performed. In order to study the boundary layer interaction between the flows over the two plates in turbulent conditions, a LES using the Vreman model is conducted. During the investigation, the distance between the two plates is modified, to evaluate how this parameter was affecting the heat transfer rate. In this research, an inlet and an outlet region are inserted above and below the region of the domain where the hot wall is located, the inlet region is necessary in order to give the possibility to the fluid to flow from the leading edge of the wall and along the wall, and the outlet region is needed in order to avoid that the boundary conditions in the upper part, strongly affect the heat exchange on the hot wall. The results of the study demonstrated that the heat transfer rate of the flow through the two plates was lower than that one over a single vertical plate. It is concluded that the lower heat transfer rate is caused by a reduced velocity gradient in the outer region of the boundary layer.

In the paper presented by Ortiz and Koloszar (2020) the natural convection heat transfer on a vertical wall is investigated, in order to enhance the turbulence in the boundary layer. In the investigation, a transition control technique is applied to promote the destabilization of the flow, in order to enhance the transition to a turbulent state. In this research, a spacing below the hot wall is added, and the scope was to facilitate incoming flow close to the leading edge of the hot plate, in this case the boundary condition below the inlet region is set to zero velocity, to force the fluid to enter from the side of the domain.

1.2 Problem Motivation

From the investigation of previous studies about similar researches, it is observed that changing the characteristics of a flat wall, leads to changes of the heat transfer rate, on a local and general level. Therefore analyzing a different configuration of a vertical wall will be the main focus of this thesis. In particular, as shown in the literature review, a wavy configuration could lead to local or general change of the heat transfer, and it is also showed that various settings of the domain can be chosen to still reach the same result of simulating the natural convection over a flat vertical wall. In this thesis, the heat transfer natural convection phenomenon on a vertical wavy wall will be investigated, and the analysis will be performed changing some parameters of the wavy wall, in order to analyze how these parameters could lead or not to an improvement of the heat transfer rate.

Problem Statement and methodology 2

2.1 Problem statement

In this thesis, different CFD simulations of the flow along a vertical wall will be performed, in order to assess if a wavy shape is a convenient modification to enhance the heat transfer. The evaluation of the performances of the different configurations analyzed in the thesis will be focused on the Nusselt number. Assessing the change of the Nusselt number along the wall and comparing the average values of the different configurations, will be crucial for understanding if an enhancement of the heat transfer is achieved.

In order to reach a clear understanding of the objective of the thesis, it is necessary to define a problem statement:

How the heat transfer rate of a vertical wall is affected when the geometry is changed from flat to wavy?

To complete the picture of the problem investigated in this report some sub-questions are useful.

- How does the Nusselt number vary along the wall?
- Does the average Nusselt number change too?
- How the amplitude of the wave is affecting the heat transfer rate?
- How the number of waves on the vertical wall is affecting the heat transfer rate?

Until the end of the study these questions will be taken as a reference, and the scope of the research will be to give a clear description of the phenomenon.

The parameter chosen to evaluate the performance of the different configurations is the Nusselt number, because it represents the enhancement of heat transfer reached with heat convection compared to heat conduction under same temperature conditions (Cengel, Klein, and Beckman, 1998), the larger the Nusselt number and the more effective is the convection.

The parameters of the simulation will be set to achieve a laminar flow. The CFD software used to set up the model is the open source software OpenFOAM.

2.2 Methodology

The following methodology is applied in order to answer the questions of the problem statement, a detailed diagram is presented in Fig. 2.1.

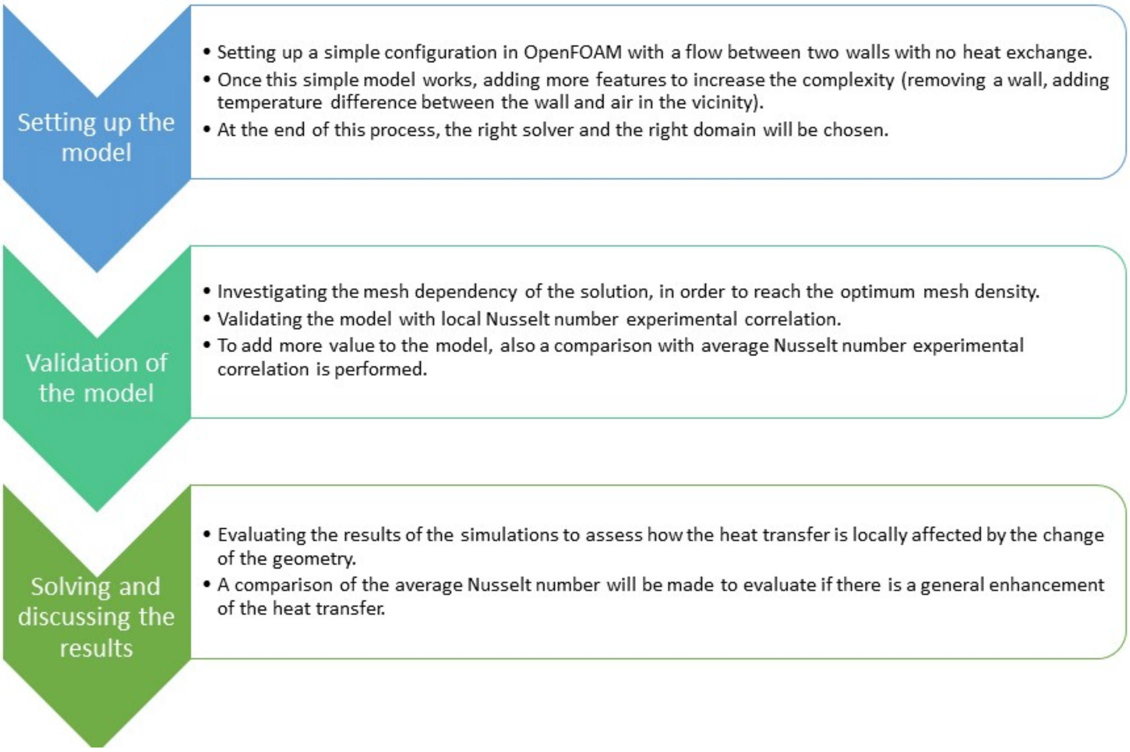

Figure 2.1: *Project methodology representation.*

As can be seen in the diagram, the first step is to construct a numerical model in OpenFOAM. Considered the complexity of the CFD software, a very simple model is made to start, in order to simulate the flow between two walls at a fixed velocity. Afterwards, more complex configurations are studied, removing one of the wall and then adding a temperature difference between the wall and the air, still keeping the flow at a fixed velocity. In the final configuration, to simulate the natural convection phenomenon, no flow velocity is imposed.

The second step will be validating the model, by comparing it with experimental correlations both for local and average Nusselt number. The last part of the thesis will be a discussion of the results of the different configurations, in order to assess if there is an enhancement of the heat transfer on a vertical wall by natural convection, motivating the phenomena observed.

Part II

Modeling

Theoretical background 3

In this chapter, the theory necessary to understand the problem investigated, will be described. The main focus will be given to the explanation of the meaning of thermal and velocity boundary layer, and their importance for the natural convection heat transfer. Afterwards, the most important non-dimensional numbers used to describe the characteristics of the flow and of the heat transfer, will be presented. In the last part, all the governing equations which are involved in the current phenomenon will be defined.

3.1 Thermal and velocity boundary layers

In this section, the thermal and the velocity boundary layer for natural convection on a flat vertical hot plate at constant temperature are described. In Fig. 3.1 there is a representation of the these boundary layers for a particular case where they both have the same thickness. As can be seen, the velocity distribution of the fluid inside the boundary layer is changing along the y direction. In particular, it is zero on the wall, then it starts to increase, until it reaches a maximum, and it starts to decrease until it reaches a value of zero on the edge of the boundary layer. Outside the velocity boundary layer, for this kind of problem, the velocity of the fluid is zero. The thermal distribution inside the thermal boundary layer is different, the maximum temperature T_s is observed on the surface. Then it starts to decrease until the edge of the thermal boundary layer, where it reaches the same temperature T_{inf} of the outside fluid. Thus it can be stated that the thickness of the velocity boundary layer δ_u for natural convection problem, is equal to the perpendicular distance from the plate to the position where a velocity equal to zero is registered. The thermal boundary layer thickness δ_T is instead equal to the perpendicular distance from the wall, to the position where a temperature equal to T_{inf} is registered.

$$\delta_u = y(u = 0) \tag{3.1}$$

$$\delta_T = y(T = T_{inf}) \tag{3.2}$$

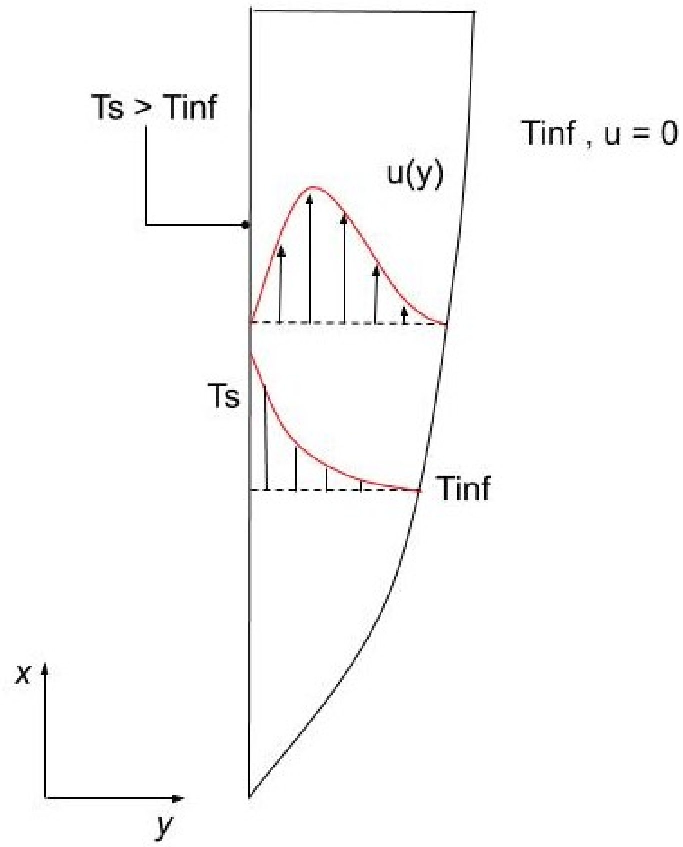

Figure 3.1: *Velocity and thermal distribution inside the boundary layer of a fluid flow over a hot flat plate, particular case where velocity and thermal boundary layer have the same thickness.*

3.2 Non-dimensional numbers

In this section, the non-dimensional numbers useful to better understand and describe the phenomena involved in the natural convection heat transfer, are described. Each of the number has a crucial characteristic, some are used to define properties of the fluid, others to describe the turbulence of the flow or the peculiarity of a particular heat transfer phenomenon. More details are presented following.

Prandtl Number

The Prandtl number is the only number, among those presented in this section, which describes the properties of the fluid. As can be seen in the following equation, the main focus is the relation between the kinematic viscosity and thermal diffusivity. This relation is very important in the natural convection, where motion of the fluid and heat transfer, are the main characteristics of the phenomenon.

$$Pr = \frac{\mu/\rho}{k/\rho C_p} = \frac{\mu C_p}{k} = \frac{\nu}{\alpha} \tag{3.3}$$

Where:

- μ is the dynamic viscosity of the fluid.
- ρ is the density of the fluid.
- C_p is the heat capacity of the fluid.
- ν is the kinematic viscosity of the fluid.
- α is the thermal diffusivity of the fluid.

The Prandtl number equation includes some parameters which affect the thermal and velocity boundary layer, it gives information on the relation between the two boundary layers during the flow. When the Prandtl number is equal to 1, the two boundary layers have same thickness, if it is above 1, then the thickness of the velocity boundary layer is greater than the thermal one, and vice-versa.

Grashof Number

The Grashof number is one of the parameter used in natural convection to define the turbulence of the fluid. In the equation below, the parameters which affect the Grashof number can be seen:

$$Gr = \frac{g\beta(T_s - T_\infty)L_c^3}{\nu^2} \tag{3.4}$$

Where:

- g is the gravitational acceleration.
- β is the volume expansion coefficient.
- L_c is the characteristic length of the geometry.

This number is defined by the ratio of the buoyancy force on the viscous force, which are the main forces that affect the fluid flow during the natural convection. The value of the Grashof number will determine the nature of the flow. Based on literature, the transition to turbulence zone, starts for Gr $= 10^8$ (Cengel, Klein, and Beckman, 1998).

Rayleigh Number

The Rayleigh number is another non-dimensional number which is often used to define the turbulence of the flow. According to theory, the transition to turbulence zone starts around Ra $= 10^9$ (Hewitt, Shires, and Bott, 1994). The equation which describes the Rayleigh number is expressed as follows:

$$Ra = Gr \cdot Pr \tag{3.5}$$

This number is dependent on the Prandtl and Grashof number. The meaning of this equation is of high importance in the description of the fluid flow, because it states that the turbulence of the flow is both the result of the characteristic of the fluid and balance of the forces acting on the fluid.

Nusselt Number

As mentioned in the Problem statement, the Nusselt number will be a crucial value for the investigation made in this thesis, because it quantifies how much the heat transfer rate is increased by the heat convection, compared to the heat conduction.

$$Nu = \frac{\dot{q}_{conv}}{\dot{q}_{cond}} = \frac{h\Delta T}{k\Delta T/L} = \frac{hL}{k} \tag{3.6}$$

Where:

- $\dot{q}_{conv}$ is the heat exchanged by convection.
- $\dot{q}_{cond}$ is the heat exchanged by conduction.
- h is the convection heat transfer coefficient.
- k is the conduction heat transfer coefficient.
- L is thickness of the fluid layer where the heat is exchanged.

In literature there are many experimental correlations, such as Bejan (2013) and Churchill and Chu (1975), which have determined the formulation of the average Nusselt number for specific conditions, and they describe the Nusselt number as a function of the Rayleigh and Prandtl number. In Bejan (2013), the Nusselt number for a vertical isothermal surface is expressed as:

$$Nu = \left\{ 0.825 + \frac{0.387Ra^{\frac{1}{6}}}{[1 + (\frac{0.492}{Pr})^{\frac{9}{16}}]^{\frac{8}{27}}} \right\}^2 \tag{3.7}$$

Where:

- Pr is the Prandtl number.
- Ra is the Rayleigh number.

In Churchill and Chu (1975) , the Nusselt number correlation for a vertical isothermal surface is the following:

$$Nu = 0.68 + \frac{0.67Ra^{\frac{1}{4}}}{[1 + (\frac{0.492}{Pr})^{\frac{9}{16}}]^{\frac{4}{9}}} \tag{3.8}$$

3.3 Governing Equations

To understand the physics of the problem investigated, it is crucial to describe the formulation of the equations for the natural convection. This formulation will match the physics of the solver used in this research, the following equations are part of the source code of the OpenFOAM solver *buoyantPimpleFoam* used to solve all the cases investigated in this thesis (Weller et al., 1998).

Conservation of Mass

The equation of conservation of mass takes in account the basic principle that the mass cannot be generated or eradicated. In the following formulation, since the solver used is transient, also the time derivative term is taken in account:

$$\frac{\partial \rho}{\partial t} + \nabla \cdot (\rho \mathbf{u}) = 0 \tag{3.9}$$

Where:

- $\mathbf{u}$ is the velocity field.
- ρ is the density field.

Conservation of Momentum

This equation describes the balance of the forces acting on a defined portion of mass. In particular, it is taken in account the contribution of the pressure, gravity and viscous forces acting on each fluid element. The expression of this equation can be seen as follows

$$\frac{\partial (\rho \mathbf{u})}{\partial t} + \nabla \cdot (\rho \mathbf{u}\mathbf{u}) = -\nabla p + \rho \mathbf{g} + \nabla \cdot (2\mu_{eff} D(\mathbf{u})) - \nabla \left(\frac{2}{3} \mu_{eff} (\nabla \cdot \mathbf{u}) \right) \tag{3.10}$$

Where:

- p is the static pressure field.
- $\mathbf{g}$ is the gravitational acceleration.
- μ_{eff} is the effective viscosity, sum of the laminar and the turbulent viscosity.

$D(\mathbf{u})$ is the strain-rate tensor, and is defined as follows:

$$D(\mathbf{u}) = \frac{1}{2} \left(\nabla \mathbf{u} + (\nabla \mathbf{u})^T \right) \tag{3.11}$$

Conservation of Energy

The key principle of this equation is to describe the rate of accumulation of energy for a specific control volume of fluid as the sum of the energy transferred to the control volume, minus the work made by control volume to the environment. Among the solver options, it is possible to choose either internal energy or enthalpy as the energy solution variable, in this case the enthalpy is chosen, thus the energy conservation equation is the following:

$$\frac{\partial(\rho h)}{\partial t} + \nabla \cdot (\rho \mathbf{u} h) + \frac{\partial(\rho K)}{\partial t} + \nabla \cdot (\rho \mathbf{u} K) - \frac{\partial p}{\partial t} = \nabla \cdot (\alpha_{eff} \nabla h) + \rho \mathbf{u} \cdot \mathbf{g} \tag{3.12}$$

Where:

- K is the kinetic energy per unit mass.
- h is the enthalpy per unit mass, defined as the sum of the internal energy and the kinematic pressure.
- α_{eff} is the effective thermal diffusivity, sum of the laminar and the turbulent thermal diffusivity.

The choice of the solver to investigate the problem of this thesis went to *buoyantPimpleFoam*, this is a transient solver which does not use the Boussinesq approximation. This solver uses the PIMPLE algorithm to control the pressure-velocity coupling, the PIMPLE algorithm is a combination of the the PISO (Pressure Implicit whit Splitting Operator) and the SIMPLE (Semi-Implicit Method for Pressure-Linked Equations) algorithm. At each iteration, it follows all the steps reported in the flowchart in Fig. 3.2.

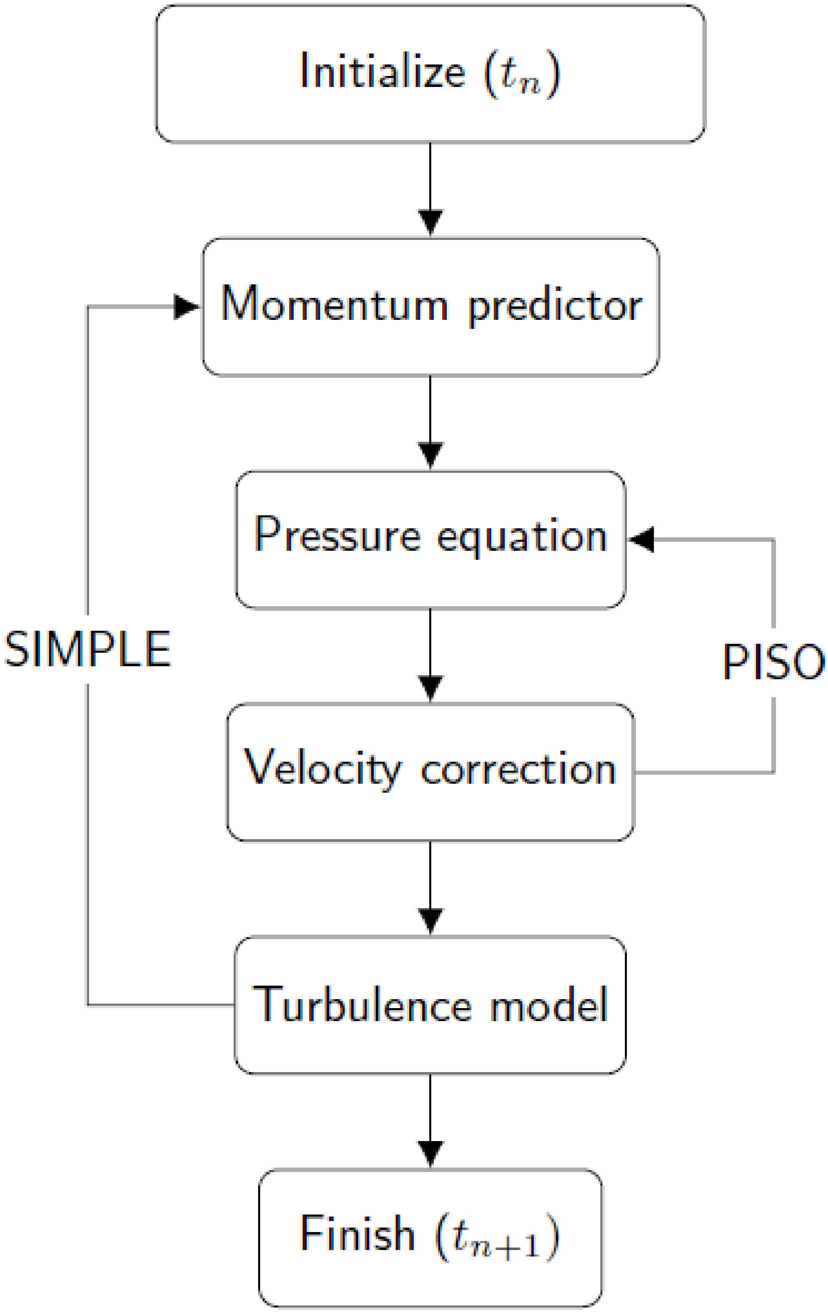

Figure 3.2: *Flowchart of the PIMPLE algorithm (Winter and Sváček, 2019) .*

Numerical Modeling 4

In the following chapter the numerical model is presented. At the beginning the model structure is described, the division in three blocks of the domain and the boundary conditions. Afterwards the grid independence study and the code validation are performed.

4.1 Model Presentation

The domain to solve the heat transfer problem of this thesis is made by three blocks, which consist of a structured mesh. Each of the block has a particular function which will be assessed more in detail during this section.

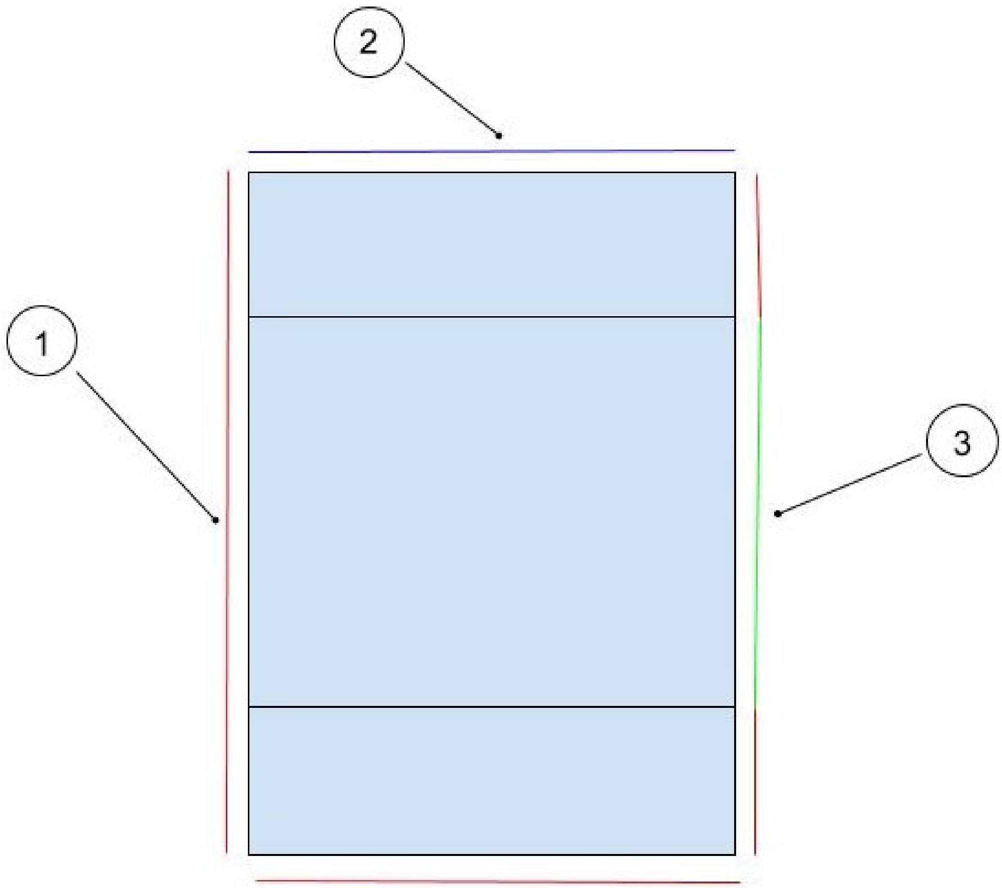

Figure 4.1: *Computational domain for all the simulations.*

The structure of the 2D domain built to analyse the heat convection through the vertical plate is presented in Fig. 4.1. The domain is divided in three blocks, the central block is where the heat exchange happens. The block under it , is made to ensure the good incoming flow close to the hot plate's leading edge. The block above instead is necessary to ensure that the boundary condition at the top, did not affect the flow adjacent to the heated plate. The choice of the boundary conditions comes after the investigation described in the Methodology, these are settings which have shown the best results, when validated whit experimental data.

Boundary 1 - Adiabatic walls

It is the boundary highlighted in red. The presence of these walls is necessary to facilitate the incoming flow at the plate edge from below. The velocity on the walls is set to zero and all the walls are adiabatic.

Boundary 2 - Inlet and Outlet patch

In this patch the fluid can pass to enter and leave the domain. In this boundary a fixed temperature T_{inf} is imposed, in order to sustain the heat exchange between the hot wall and the cooler fluid entering the domain. It is worth to specify that the starting temperature for all the fluid in the domain was also equal to T_{inf}. In this patch a pressure boundary is imposed, a constant mean value of the pressure is fixed. The kind of boundary used, extrapolates the value of the pressure to the patch using the near-cell values and then regulates the distribution of the pressure to match the specified mean value.

Boundary 3 - Hot wall

On the hot surface, the temperature is kept fixed to a value $Ts > T_{inf}$. In this way the temperature of the wall can continuously heat up the cooler fluid entering the domain. At the wall no-slip condition are imposed, in order to facilitate the formation of the boundary layer along the hot wall.

In this analysis, only laminar cases are investigated, this means that for all the simulations performed, the conditions Gr $< 10^8$ and Ra $< 10^9$ are satisfied. Considered that, it is chosen to not to use any RANS turbulent model, and a LES model was considered of too high computational cost for the purpose of this study. In the *turbulenceproperties* OpenFOAM dictionary, the simulation type is set to *laminar*. For all the cases, the time step during the simulations was kept to 0.002 seconds, in order to ensure the convergence, and that the Courant number remained below acceptable values. The grading of the mesh is set in order to assure that the width of the cells close to the hot wall is ten times smaller than the width of the cells on the extreme left side. This is done to provide a good density of cells where the heat exchange happens. On the other side, considered that for all the simulations the flow is laminar, it was not considered necessary to have a particularly high density of cells in the area of the hot wall, thus the grading was never set higher than the value mentioned.

4.2 Grid independence study

It is important that the solution of the model is not strongly dependant from the number of cells used in the computational domain. Therefore a grid independence study is made, by looking at the variation of the average Nusselt number along the vertical flat wall, keeping the Grashof number fixed at $6.8 \cdot 10^5$.

The study is made starting from a relatively low cell density, with a number of 9375 cells. From this number, the number of cells is doubled at each step, until a maximum of 372000 cells. As can be seen in Fig. 4.2, by increasing the number of cell from 84375 to 372000 the Nusselt number changes from 13.786 to 13.802, that is an increasing of 0.12%.

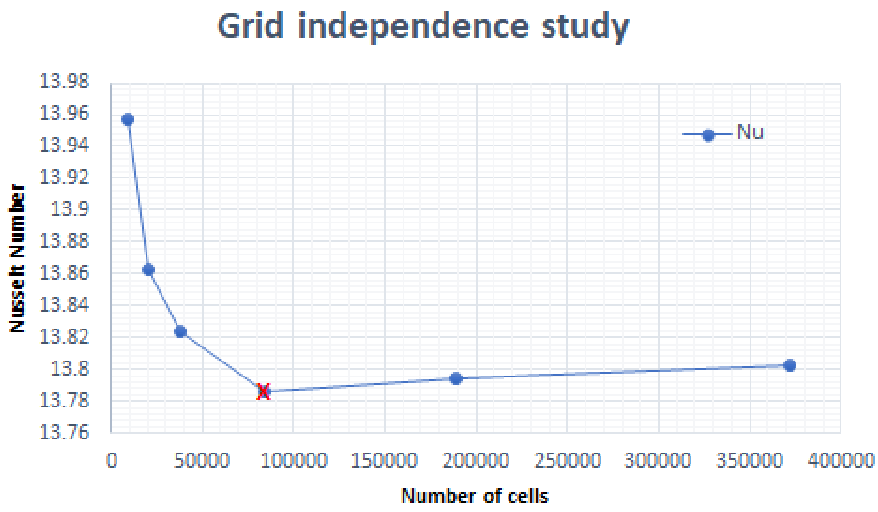

Figure 4.2: *Grid independence study at* $Gr = 6.8 \cdot 10^5$.

A substantial amount of computational time is spent every time the mesh size is doubled. Since the change in the Nusselt number is considered acceptable, a mesh of 84375 cells is chosen. It is observed that smaller mesh sizes would also give an acceptable change of Nusselt number, but the choice of 84375 is considered optimal, because the calculation time is considered tolerable.

4.3 Code validation

The numerical model set up in this study will be validated with experimental data presented in literature. The validation of the code will be performed for the flat vertical wall configuration. Many investigations have been made on Nusselt number, therefore different ways to validate the present research are available. It is chosen to analyze both the average and local distribution of the Nusselt number, to add more value to this study. In order to calculate the heat flux at the hot wall, it is used an OpenFOAM function object called *wallheatflux*, which allows to calculate the value of the heat flux, at a specified patch. All the simulations are performed keeping the Prandtl number at 0.7.

Validation by average Nusselt number experimental correlation

As stated in Sec. 3.2, many experimental correlations are presented in literature, these can be useful for the validation of the model used in the present work. In particular, the experimental correlations already described in Sec. 3.2 by Bejan (2013) and Churchill and Chu (1975), are investigated.

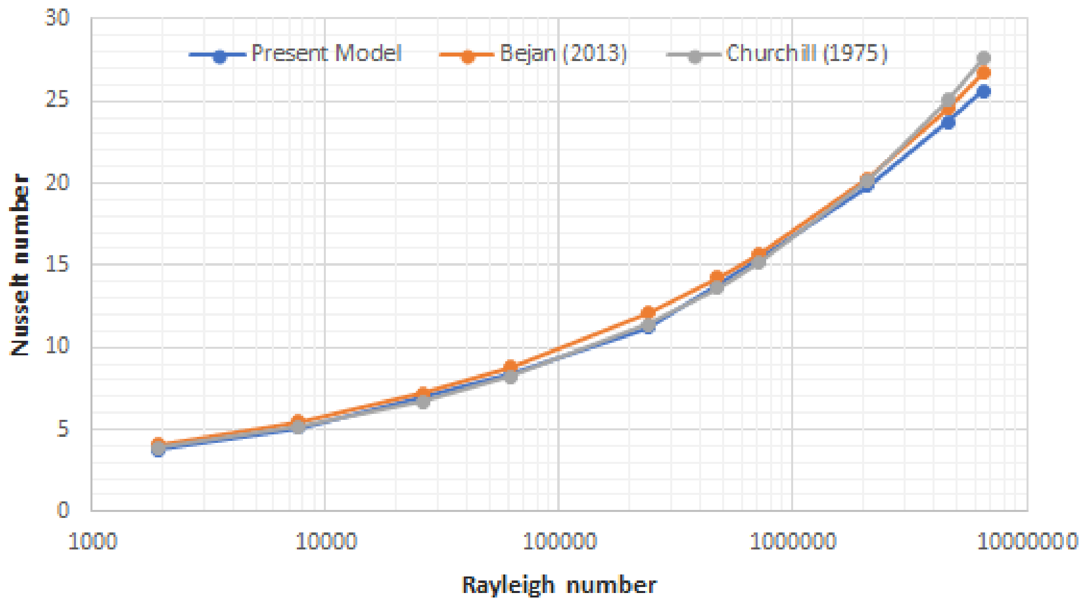

Figure 4.3: *Average Nusselt number code validation.*

As can be seen in Fig. 4.3, the present model shows quite a good agreement with Churchill and Chu (1975) and a fair good agreement with Bejan (2013). For higher Rayleigh numbers, closer to the transition to turbulent zone, the Nusselt value is slightly underestimated, compared to the experimental results.

Validation by local Nusselt number semi-analytical correlation

The local distribution of the Nusselt number is compared with the correlation suggested by Ostrach (1952), in this correlation the local Nusselt number is a function of the local Grashof number and the Prandtl number. Local Grashof number and local Nusselt number are defined as follows:

$$Gr_y = \frac{g\beta(T_s - T_\infty)y^3}{\nu^2} \qquad (4.1)$$

$$Nu_y = \frac{\dot{q}_{conv}}{\dot{q}_{cond}} = \frac{\dot{q}_{conv}y}{k\Delta T} \qquad (4.2)$$

Where y is the distance between the point at the coordinate y and the leading edge of the wall (where y = 0). The equation proposed by Ostrach (1952) can be seen following:

$$Nu_y = \left(\frac{Gr_y}{4}\right)^{\frac{1}{4}} \cdot g(Pr) \tag{4.3}$$

Where g(Pr) is calculated with the following equation:

$$g(Pr) = \frac{0.75Pr^{\frac{1}{2}}}{\left(0.609 + 1.221Pr^{\frac{1}{2}} + 1.238Pr\right)^{\frac{1}{4}}} \tag{4.4}$$

In Fig. 4.4, the plot of the local Nusselt number against the local Grashof number, for the present model and for the correlation proposed by Ostrach (1952) can be seen.

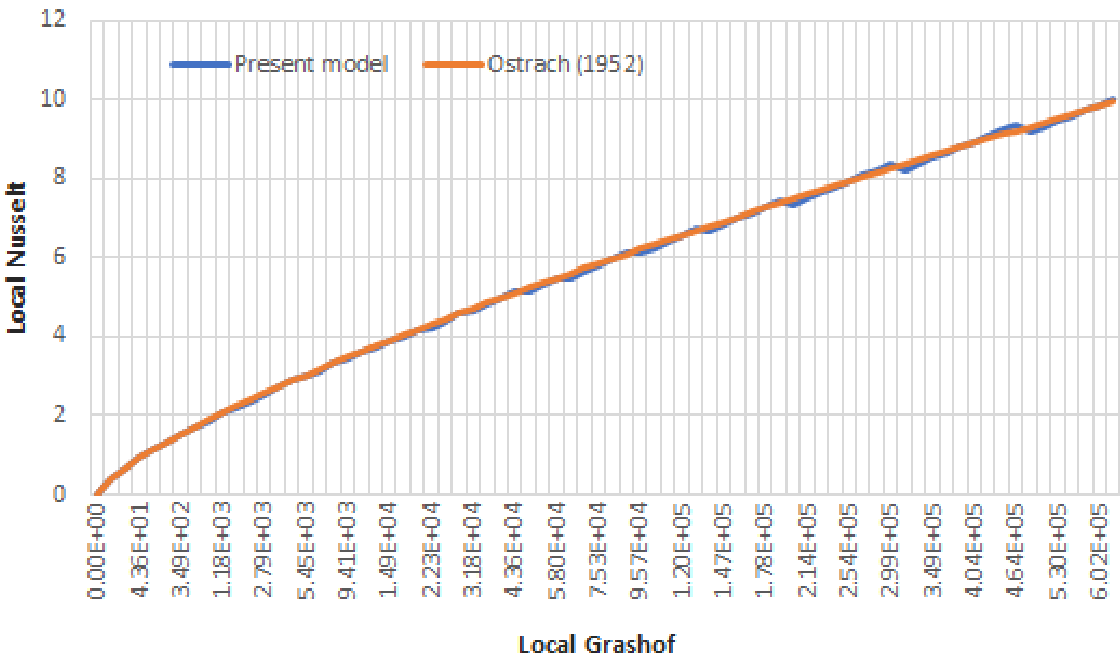

Figure 4.4: *Local Nusselt number code validation.*

It can be observed that the model shows a very good agreement with the theory proposed, in particular the two trends considerably match for the first half. For higher Grashof values, there is a slight difference, probably caused by a low grid density, not enough sufficient to catch all the variations of Nusselt number along the plate.

Part III

Results

Results 5

The goal of this chapter is to present the structure of the results, in order to highlight which are the characteristics of the flow along the different vertical plates assessed. During the investigations, the Grashof and Prandtl number are respectively fixed to $Gr = 6.8 \cdot 10^5$ and $Pr = 0.7$. In this thesis two different analysis will be performed, in the first one, the dimension of some parameters of the wave shape on the vertical wall will be changed. In the second one, the number of waves on the vertical wall will be changed, keeping fixed the length of the wall H and the ratio of the parameters of the wave. These parameters will be described in the next section.

5.1 First analysis

In this section, the description of the first investigation and its results are presented, the temperature and the velocity fields will be studied, to understand how these parameters affect the heat transfer.

5.1.1 Geometry description

In Fig. 5.1 is presented the basic structure of the wavy geometry, during the study the L/d ratio is modified in order to analyze how the flow and the heat transfer changes when the geometry features are changed. Four different L/d values are investigated, always doubling the value, starting from 5.

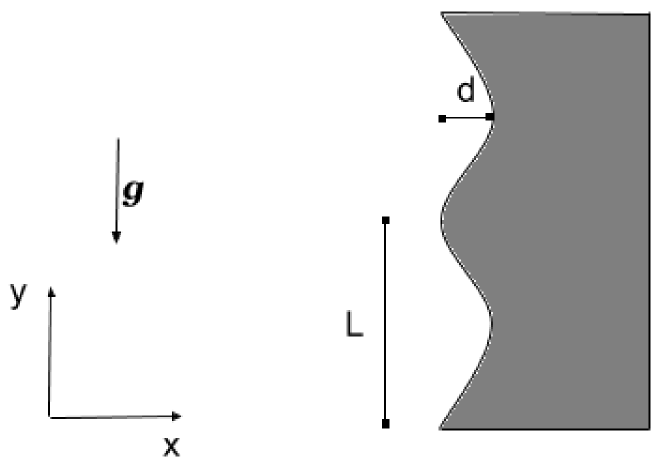

Figure 5.1: *Geometry parameters changed for the first investigation.*

5.1.2 Simulation results

In this section the results of all the cases of the first investigation are presented. In order to see how the temperature and the velocity of the flow during natural convection are developed and how they relate to each other.

Temperature

The non-dimensional temperature fields for all the four configurations can be seen in Fig. 5.2. Starting from the highest to the lowest L/d value.

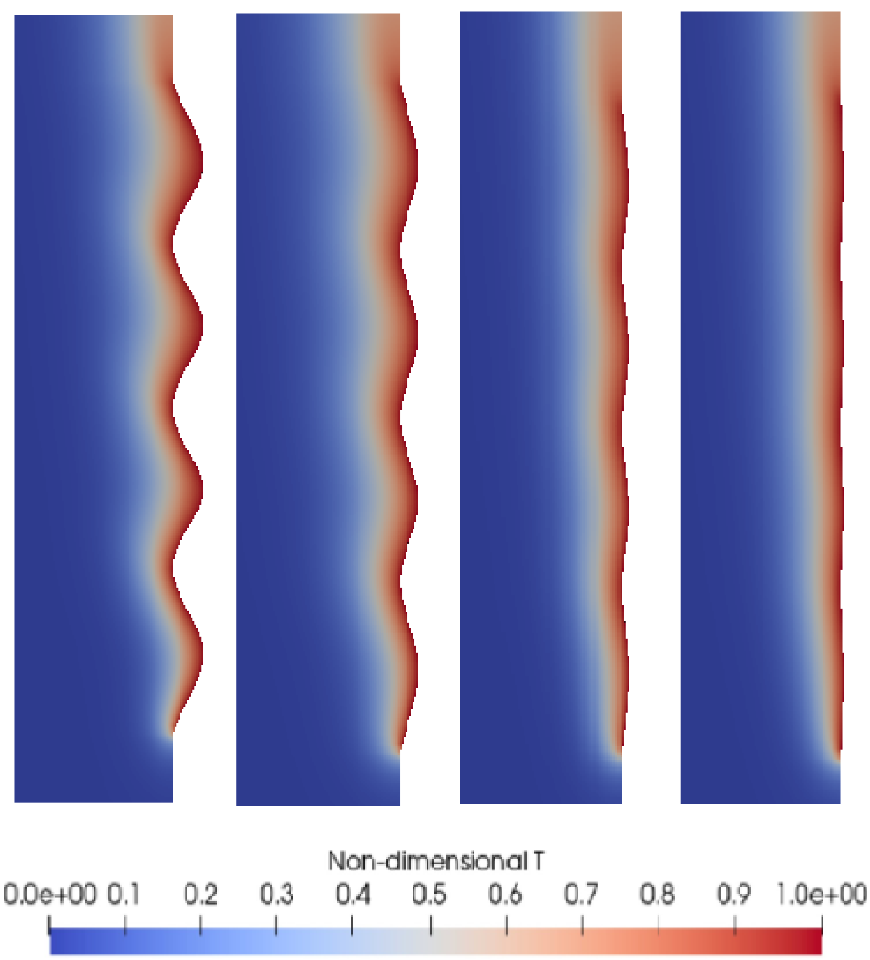

Figure 5.2: *Non-dimensional temperature field of the four geometries studied in the first investigation. From left to right, the L/d value is respectively equal to 5, 10, 20, 40.*

From the figure above it is remarkable the concentration of the hot air in the vicinity of the heated wall, it is important to notice that only the wavy part is heated up, thus the hot fluid on the upper part of the right side is hot air heated up which is going up, outside of the domain. It is noticeable that for lower L/d values, there is a slightly higher concentration of hot air in the vicinity of each wave.

Velocity

The non-dimensional velocity fields for all the configurations investigated is presented in In Fig. 5.3.

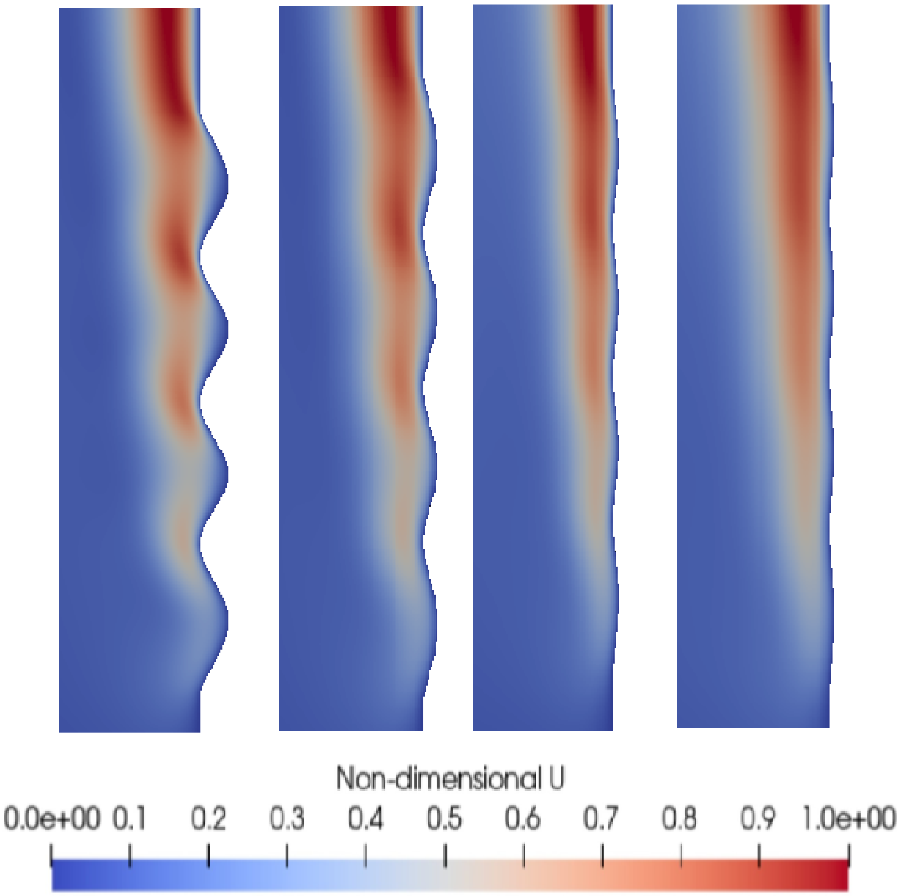

Figure 5.3: *Non-dimensional velocity field of the four geometries studied in the first investigation.*

The most interesting aspects of the velocity fields presented above are the areas at the end of each wave, where the fluid is strongly accelerated. It can be noticed that the acceleration is quite remarkable in particular for lower L/d values. The higher curvature emphasizes the contribution of the angular acceleration at the end of each wave, but this brings also a higher deceleration when entering each wave. As a consequence, some dead zones are formed, where the average velocity of the fluid is consistently lower.

5.2 Second analysis

In this section, the number of waves along the vertical wall will be changed, keeping fixed the length of the hot wall H and the ratio $L/d = 20$. As it was done in the previous section, the temperature and the velocity fields will be presented following.

Temperature

In Fig. 5.4 the non-dimensional temperature field of the four wavy geometries with different number of waves can be seen.

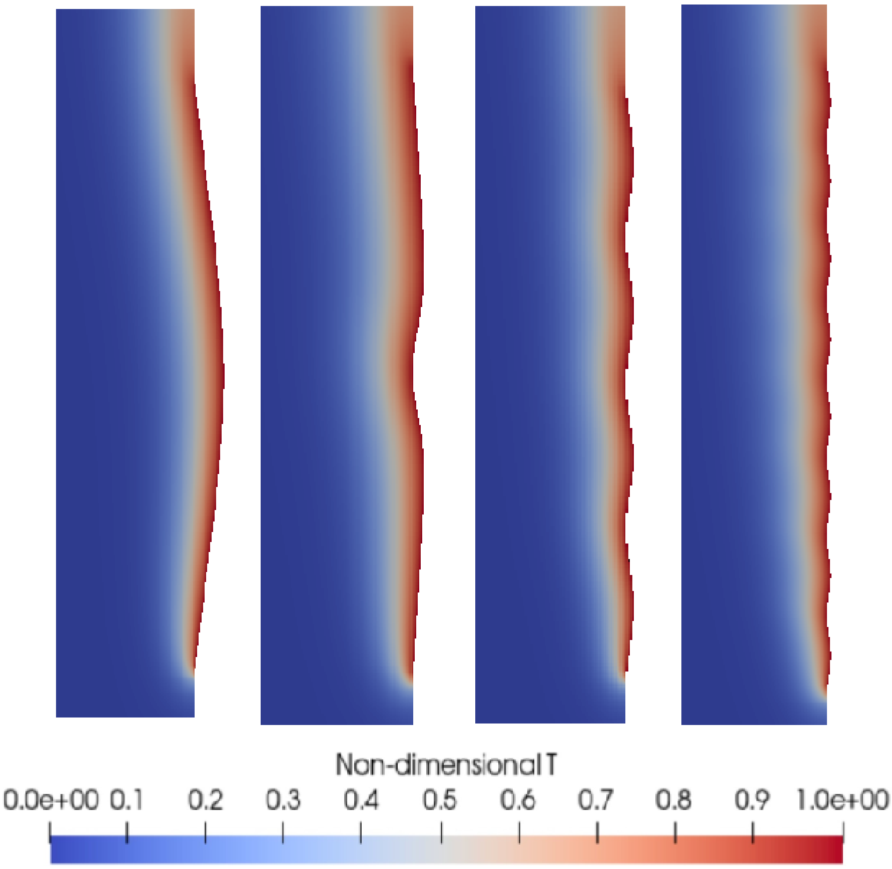

Figure 5.4: *Non-dimensional temperature field of the four geometries studied in the second investigation. From left to right, the number of waves is respectively equal to 1, 2, 4, 8.*

The characteristics of the temperature fields are not so different than the first investigation. Some similarities can be seen, with the flow of the hot air going upwards, and hotter zones in the concave part of the waves. It is worth to notice that the temperature fields of the second investigation, do not present relevant difference among each other, as instead was happening in the first investigation.

Velocity

In Fig. 5.5 the non-dimensional velocity fields of the second investigation can be observed.

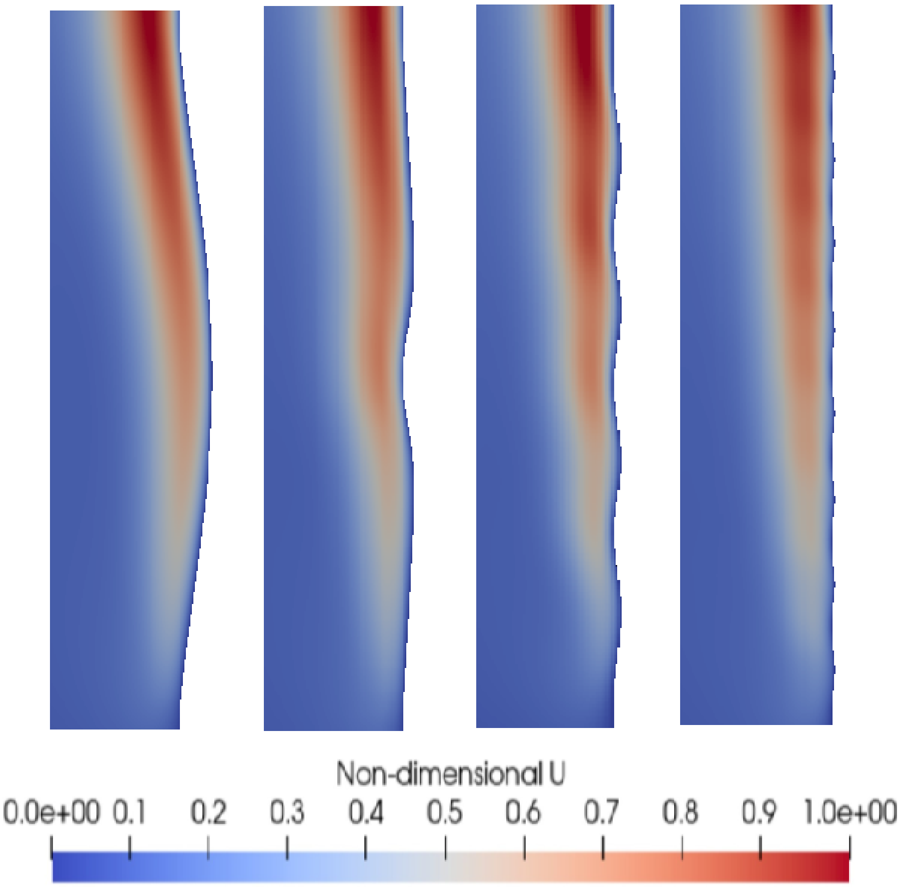

Figure 5.5: *Non-dimensional velocity field of the four geometries studied in the second investigation.*

The velocity fields presented in Fig. 5.5 show quite similar characteristics to each other, some acceleration zones can be seen in the proximity of the end of each wave. Some areas of lower velocity magnitude are more evident for the 2 and 4 waves configuration. The one wave configuration shows quite a regular pattern while it seems that 8 waves configuration has too small waves, which do not seem to affect much the flow. Further analysis of this phenomena are made in the next chapter.

Discussion of the results 6

In this chapter the results of the simulations will be discussed. The variation of the local heat transfer will be assessed, evaluating how the local Nusselt number is changing along the hot vertical plate. Afterwards a global evaluation will be performed too, observing how the average value of the Nusselt number changes, for the different configuration studied in this work. At the beginning, the first investigation is presented, where the amplitude of the wave is changed. After that, the local and the average variation of the Nusselt, changing the number of the waves.

6.1 First investigation

In this section the local variation of Nusselt number is assessed. In the post-processing phase of the CFD study, the convection heat flux on the hot wall is calculated, then the equation 4.2 is used to calculate the local Nusselt number on each cell of the vertical heated wall. Where q_{conv} is the heat convection on the cell at height y, and the thermal conductivity k is calculated using the Prandtl number definition, as follows:

$$k = \frac{\mu C_p}{Pr} \tag{6.1}$$

In Fig 6.2 the trends of the local Nusselt number for the different configurations of the first investigation can be seen.

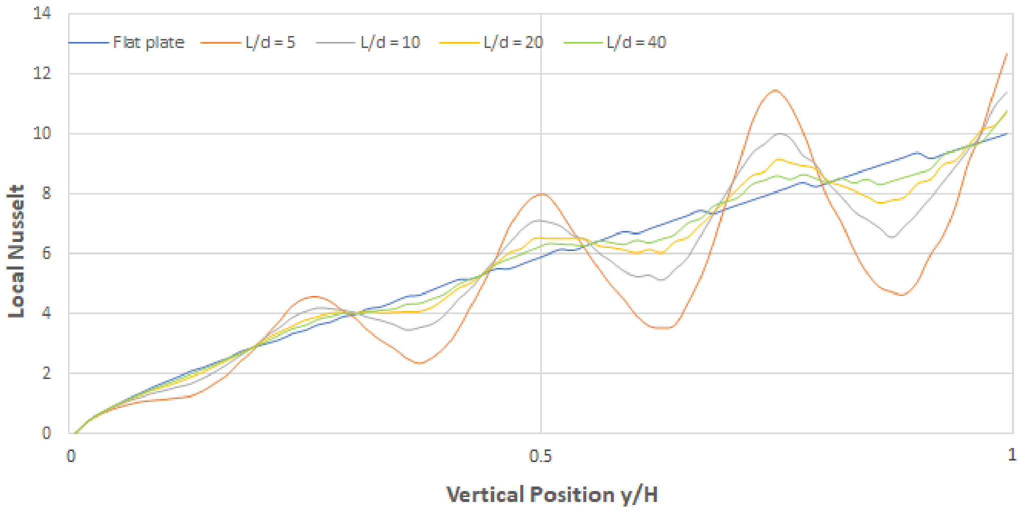

Figure 6.1: *Plot of the local Nusselt number along the hot vertical wall of height H, changing the L/d ratio.*

As can be seen in the graph, for all the wavy geometries, the local Nusselt number follows a wavy trend. In particular, it can be observed that the value reaches a local minimum every time the flow enter a new wave, and it reaches a local maximum at the end of the wave. As stated and showed in Sec. 5.1, when the fluid flow enters each wave, the local average velocity is decreased, and the flow is accelerated every time is leaving the wave. The acceleration of the fluid leads to a local increasing of the Nusselt number, because the higher is the velocity of the flow and the higher is the convection heat transfer rate. For higher L/d values, minor changes in local Nusselt number are observed. In fact, looking at the velocity field of Fig. 5.3, the lower is the L/d and less evident are the changes of the velocity distribution.

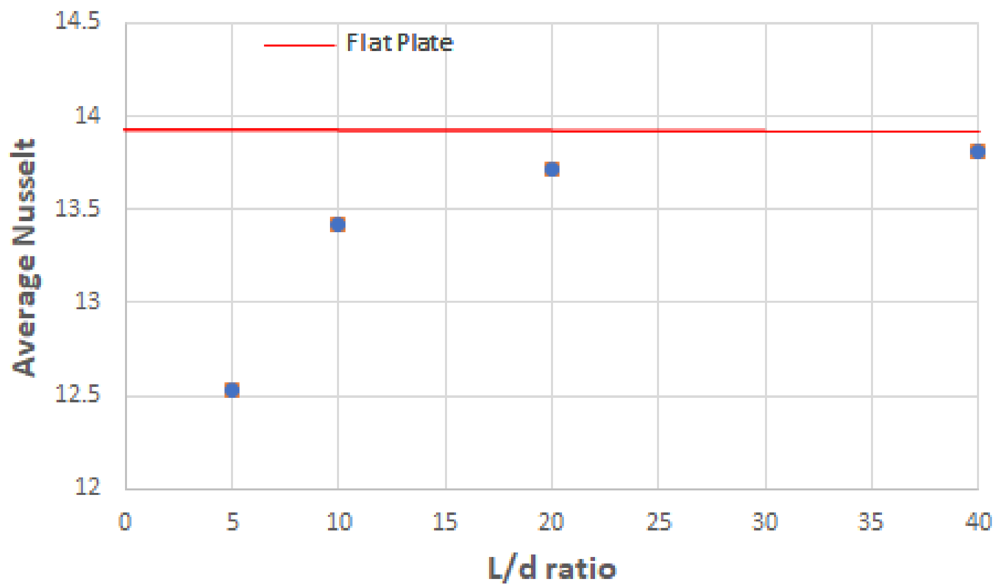

Figure 6.2: *Average Nusselt number values for the first investigations.*

In Fig. 6.2 the average value of the Nusselt number for all the configurations of the second investigation is plotted. It can be observed that increasing the L/d ratio, the Nusselt number tends to approach the value of the vertical flat plate, but for all the configurations the Nusselt number is lower. It can be concluded that this modification does not improve the overall heat transfer rate.

6.2 Second investigation

In this section, the same evaluations made in the previous one will be made, to assess what kind of changes are observed in the local and the average Nusselt number, if the number of waves along the vertical is changed.

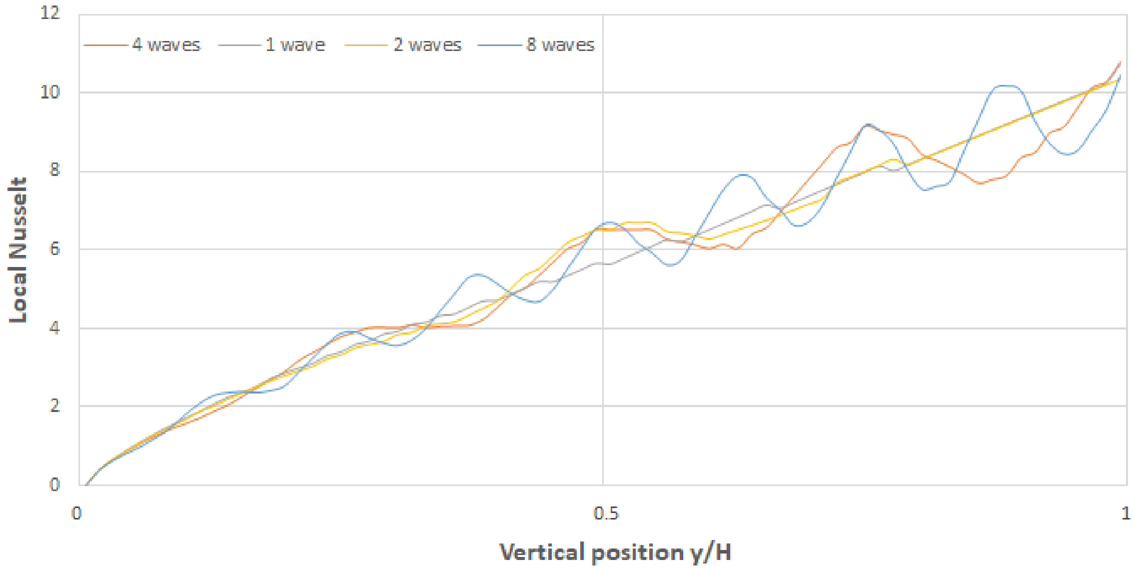

Figure 6.3: *Plot of the local Nusselt number along the hot vertical wall of height H, changing the number of waves along the wall.*

In Fig 6.3 the variations of the local Nusselt number for the second investigation can be seen. In this case, the magnitude of the changes among the different configuration is lower than in the previous analysis. The maximum and minimum peaks of the waves of the trends are also similar. This means that locally, the L/d ratio, affects the local value of the Nusselt number, more than the wavelength of the wave. In other words, the L/d value gives a higher contribution to the local acceleration of the fluid, which then brings to a higher local variation of the Nusselt number.

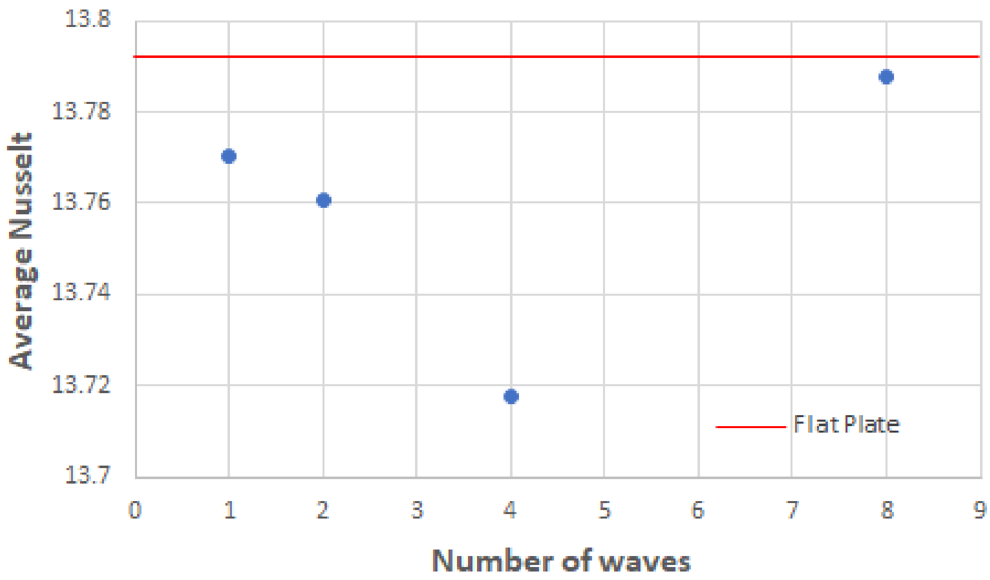

Figure 6.4: *Average Nusselt number values for the first investigations.*

In Fig. 6.4 the average values of the Nusselt number for the second analysis can be observed. As it happened in the previous case, also in this one, none of the values of the different configurations is higher than the value of the vertical flat plate. The smaller changes in magnitude observed in the local study compared to the previous case, are also evident in this evaluation, where the differences among the average Nusselt number of the different configurations are smaller. It can be concluded that modifying the number of waves on a vertical wall, is not very effective if remarkable changes of the local Nusselt number want to be achieved, and also that it does not bring an improvement of the total heat transfer rate compared to the flat vertical wall.

7 Conclusion

The natural convection on a vertical wall is studied, in order to investigate if a change of the geometry of the vertical wall could affect the heat transfer rate. It is chosen to study different wavy geometries, in order to assess how the heat transfer rate is affected by the choice of the parameters modified in this study. In particular, two investigations are performed, in the first one the amplitude of the waves is modified, in the second one the number of the waves along the wall is changed, keeping fixed the amplitude and the length of the wall.

Following the analysis of the literature review, the domain to simulate the heat exchange on the vertical wall is created. In order to ensure a good incoming flow close to leading edge of the hot plate, a region in the domain is added below the region where the hot plate is located. Then also a region above the hot plate is added, to ensure that the heat exchange on the hot wall, was not strongly affected by the boundary conditions above the hot plate.

To evaluate the heat transfer rate of all the configurations studied in this thesis, the Nusselt number value variation is analyzed. The investigation is performed on a local and overall level. It is observed that along the wavy wall, the Nusselt number changes following a wavy trend, it increases when the flow is passing close to the internal peak of each wave, and it decreases when it is flowing close to an external peak of the wave. The local maximum and minimum of the Nusselt number, are corresponding also to local acceleration and deceleration of the fluid flow along the wall. The variation of the Nusselt number along the wall is more emphasized when the amplitude of the waves is higher. It is noticed that when the number of waves is changed but the amplitude of the waves is kept constant, the local peaks of the Nusselt number along the wall are very similar, showing that for a local control of the heat exchange, varying the amplitude of the wave, is more effective than changing the number of the waves along the wall.

It is concluded that, all the waves configuration assessed in this thesis, showed a local and periodical increasing and decreasing of the heat transfer rate, compared to the flat vertical wall configuration. Looking at the average value of the Nusselt number, the flat vertical wall registers always a higher value when compared to all the other geometries studied. Concluding that, for the parameters chosen in this study, the flat vertical wall has the highest overall heat transfer rate.

Bibliography

Bejan, Adrian (2013). *Convection heat transfer*. John wiley & sons.

Cengel, Yunus A, Sanford Klein, and William Beckman (1998). *Heat transfer: a practical approach*. Vol. 141. McGraw-Hill New York.

Churchill, Stuart W and Humbert HS Chu (1975). "Correlating equations for laminar and turbulent free convection from a vertical plate". In: *International journal of heat and mass transfer* 18.11, pp. 1323–1329.

Das, Prodip Kumar and Shohel Mahmud (2003). "Numerical investigation of natural convection inside a wavy enclosure". In: *International Journal of Thermal Sciences* 42.4, pp. 397–406.

Hærvig, Jakob, Anna Lyhne Jensen, and Henrik Sørensen (2019). "Can Natural Convection on Smooth Vertical Plates in the Laminar Regime be Improved by Adding Forward Facing Triangular Roughness Elements?" In: *Proceedings of the Asme-Jsme-Ksme Joint Fluids Engineering Conference 2019*.

Hewitt, Geoffrey Frederick, George L Shires, and Theodore Reginald Bott (1994). *Process heat transfer*. Vol. 113. CRC press Boca Raton, FL.

Kogawa, Takuma et al. (2016). "Large eddy simulation of turbulent natural convection between symmetrically heated vertical parallel plates for water". In: *International Journal of Heat and Mass Transfer* 101, pp. 870–877.

Ortiz, Agustín Villa and Lilla Koloszar (2020). "Application of numerical transition control method to enhance turbulence in a natural convection boundary layer over a vertical heated plate". In: *Computers & Fluids* 199, p. 104417.

Ostrach, Simon (1952). *An analysis of laminar free-convection flow and heat transfer about a flat plate parallel to the direction of the generating body force*. Tech. rep. National Aeronautics and Space Administration Cleveland Oh Lewis Research Center.

Tanda, Giovanni (1997). "Natural convection heat transfer in vertical channels with and without transverse square ribs". In: *International journal of heat and mass transfer* 40.9, pp. 2173–2185.

Weller, Henry G et al. (1998). "A tensorial approach to computational continuum mechanics using object-oriented techniques". In: *Computers in physics* 12.6, pp. 620–631.

Winter, Ondřej and Petr Sváček (2019). "Numerical simulation of flow induced airfoil vibrations with large amplitudes". In: *Programs and Algorithms of Numerical Mathematics*, pp. 186–194.